Control of dengue virus in the midgut of Aedes aegypti by ectopic expression of the dsRNA-binding protein Loqs2

Roenick Proveti Olmo, Alvaro G. A. Ferreira, Tatiane C. Izidoro-Toledo, Eric R. G. R. Aguiar, Isaque Joao da Silva de Faria, Kátia P. R. de Souza, Kátia P. Osório, Lauriane Kuhn, Philippe Hammann, Elisa Goncalves de Andrade, et al.

Control of Dengue virus in the midgut of *Aedes aegypti* by ectopic expression of the dsRNA binding protein Loqs2

Roenick P. Olmo[1,2], Alvaro G. A. Ferreira[1], Tatiane C. Izidoro-Toledo[1], Eric R. G. R. Aguiar[1,2], Isaque J. S. de Faria[1,2], Kátia P. R. de Souza[1], Kátia P. Osório[1], Lauriane Kuhn[3], Philippe Hammann[3], Elisa G. de Andrade[1], Yaovi Mathias Todjro[1], Marcele N. Rocha[4], Thiago H. J. F. Leite[1], Siad C. G. Amadou[1], Juliana N. Armache[1], Simona Paro[2], Caroline D. de Oliveira[4], Fabiano D. Carvalho[4], Luciano A. Moreira[4], Eric Marois[2], Jean-Luc Imler[2], João T. Marques[1,2]*

[1]Department of Biochemistry and Immunology, Instituto de Ciências Biológicas, Universidade Federal de Minas Gerais, Belo Horizonte/MG, 31270-901, Brazil.

[2]Université de Strasbourg, CNRS UPR9022, Inserm U1257, 67084 Strasbourg, France.

[3]Plateforme Protéomique Strasbourg-Esplanade FRC 1589, Institut de Biologie Moléculaire et Cellulaire, 67084 Strasbourg, France.

[4]Mosquitos Vetores: Endossimbiontes e Interação Patógeno-Vetor, Instituto de Pesquisas René Rachou - Fiocruz, Belo Horizonte/MG, 30190-002, Brazil.

*e-mail: jtm@ufmg.br

Dengue virus (DENV) is an arbovirus transmitted to humans by *Aedes* mosquitoes[1]. In the insect vector, the small interfering RNA (siRNA) pathway is an important antiviral mechanism against DENV[2-5]. However, it remains unclear when and where the siRNA pathway acts during the virus cycle. Here, we show that the siRNA pathway fails to efficiently silence DENV in the midgut of *Aedes aegypti* although it is essential to restrict systemic replication. Accumulation of DENV-derived siRNAs in the midgut reveals that impaired silencing results from a defect downstream of small RNA biogenesis. Notably, silencing triggered by endogenous and exogenous dsRNAs remained effective in the midgut where known components of the siRNA pathway, including the dsRNA binding proteins Loquacious and r2d2, had normal expression levels. We identified an *Aedes* specific paralog of *loquacious* and *r2d2,* hereafter named *loqs2,* which is not expressed in the midgut. Loqs2 interacts with Loquacious and r2d2 and is required to control systemic replication of DENV and also Zika virus (ZIKV). Furthermore, ectopic expression of Loqs2 in the midgut of transgenic mosquitoes is sufficient to restrict DENV replication and dissemination. Together our data reveal a mechanism of tissue specific regulation of the mosquito siRNA pathway controlled by Loqs2.

Previous studies observed production of DENV-derived siRNAs and piwi-interacting RNAs (piRNAs) in infected mosquitoes and suggested that different RNA interference (RNAi) mechanisms were important to control virus replication[2,3,6,7]. In order to investigate the activation of RNAi by DENV infection in mosquitoes, we first analyzed different concentrations of the virus in the blood meal (Supplementary Fig. 1a,b). Using 10^7 PFU/mL of virus, we observed that 100% of individual mosquitoes had detectable virus at 1 and 2 days post feeding (dpf) (Fig. 1a). This likely corresponds to the virus inoculum in the blood meal since the amount of viral RNA decreased until 4 dpf when mosquitoes have completed blood digestion[8]. At this point, viral RNA could not be detected in some mosquitoes, suggesting that they had cleared the virus (defined

as undetectable group). Other individuals had detectable levels of viral RNA but below the lowest signal detected at 2 dpf (low viral load group). The third group of mosquitoes had viral RNA levels similar or higher than the inoculum detected at 2 dpf (high viral load group). At 8 and 14 dpf, we noted a decrease in mosquitoes in the low viral load group and a concomitant increase in mosquitoes with no detectable viral RNA (Fig. 1a). The antigenome of DENV could not be amplified by strand-specific RT-PCR in the "undetectable" group, and only trace amounts were observed at the latest time points in the "low" group (Fig. 1b). By contrast, the DENV antigenome was readily detectable as early as 4 dpf in the "high" group, indicating that the virus was actively replicating in these individuals. We interpret that these different groups of mosquitoes represent individuals that eliminated the virus ("undetected"), are in the process of eliminating/controlling the virus ("low viral load") or were productively infected ("high viral load").

To determine if RNAi contributes to clearance/control of the virus, we deep-sequenced small RNAs from the 3 groups of mosquitoes at different time points (Fig. 1c-e). Mosquitoes given a non-infectious blood meal were used as controls (Fig. 1f). Production of DENV-derived siRNA (21 nt accumulation with symmetrical distribution between sense and antisense strands) was only observed in individuals with high viral load (Fig. 1c). Production of virus-derived siRNAs in these mosquitoes increased with time and correlated with viral load ($r=0.92$, $p=0.0079$). A few dozen reads per million (RPM) of virus-derived small RNAs were detected throughout the kinetics of infection in individuals with low viral load, but these had a broad size profile suggestive of random degradation products[9] (Fig. 1d). Mosquitoes from the undetectable group had background amounts of virus-derived small RNAs similar to the uninfected control group in the order of less than 10 RPM (Fig. 1e,f). We conclude that the siRNA pathway was likely not responsible for elimination or control of DENV in these mosquitoes where the infection was presumably restricted to the midgut[10,11]. Of note, the few observed DENV-derived small RNAs with sizes matching that of piRNAs (24-29 nt) lacked canonical characteristics of the piRNA pathway such as a 5' U

enrichment and 10-nt overlap between strands as a result of the ping-pong mechanism[9]. We next injected the virus into the hemocoel of mosquitoes to monitor the response to direct systemic infection. In this case, all mosquitoes became infected and the viral load increased similarly over time even at the lowest dose (Supplementary Fig. 1c). Mosquitoes injected with 160 PFU, where viral replication was kinetically similar to individuals fed with 10^7 PFU/mL (Compare Fig. 1a and Fig. 1g), showed production of DENV-derived siRNAs as early as 1 day post injection (dpi) (Fig. 1h). This response increased proportionally to viral RNA levels (r=0.99, *p*=0.0052) (Fig. 1h). The similarity in the small RNA profiles observed between the high viral load group after a blood meal and the injection group suggests that the siRNA pathway is strongly activated once the virus disseminates systemically. Here again, we did not observe production of virus-derived piRNAs (Fig 1h).

We next assessed the impact of mosquito RNAi on different outputs of DENV infection (Fig. 2a) by silencing AGO2, the core component of the siRNA induced silencing complex[12]. Injection of dsRNA complementary to AGO2 (dsAGO2) led to 85.7% silencing of this gene in the midgut compared to a control targeting the firefly *Luciferase* gene (dsFLUC) (Supplementary Fig. 2a). Despite efficient silencing, dsAGO2 treated mosquitoes did not show an increase in viral load nor prevalence of infection in the midgut at 3 and 4 dpf (Fig. 2b,c). To directly monitor viral replication in the midgut, we used immunofluorescence microscopy with antibodies recognizing the viral envelope (E) protein (Supplementary Fig. 2b). Quantification of imaging results showed that numbers of DENV infection foci per midgut did not increase in dsAGO2 treated mosquitoes compared to controls and was even slightly decreased (Fig. 2d). Furthermore, there was no difference in the size of the infection foci between dsAGO2 and control mosquitoes (Fig. 2e). These results confirm that the siRNA pathway has limited impact, if any, on the control of early DENV infection or replication in the mosquito midgut.

We next analyzed the carcasses of the same mosquitoes that were infected by an infectious blood meal. At 3 and 4 dpf, there was no significant difference between viral load in the carcass of control and dsAGO2 treated mosquitoes (Fig. 2f). Control and dsAGO2 treated mosquitoes also showed little systemic dissemination of DENV as indicated by the low prevalence of infection in the carcass (Fig. 2g). In contrast, dsAGO2 treated mosquitoes had significantly higher prevalence of disseminated infection at 8 dpf, even though viral RNA levels were not significantly increased at this time point (Fig. 2f,g). These results suggest that AGO2 controls viral replication upon systemic dissemination. Indeed, upon DENV injection into the hemocoel of mosquitoes, which results in direct systemic infection, viral load was significantly increased in dsAGO2 treated individuals (Fig. 2h). Altogether, our findings reveal that the siRNA pathway controls systemic infection by DENV but fails to efficiently restrict the virus in the midgut.

Curiously however, the siRNA pathway appears to be functional in the midgut since *AGO2* expression is efficiently silenced by injected long exogenous dsRNA (Supplementary Fig. 2a). Accordingly, core components of the pathway (*Dcr-2*, *r2d2*, *AGO2, Hen1* and *loqs-RA*) are expressed in the midgut at similar or higher levels than in whole mosquitoes (Fig. 3a). Furthermore, transposable elements (TEs), which are controlled by the endogenous siRNA pathway in somatic tissues of insects[13], were significantly upregulated in the midgut of dsAGO2 treated mosquitoes compared to controls (Fig. 3b). These results suggest that the siRNA pathway is fully functional in the midgut when activated by endogenous and exogenous sources of dsRNA.

To test whether DENV is resistant to AGO2 mediated gene silencing in the midgut, we engaged the exo-siRNA pathway by injecting mosquitoes with dsRNA targeting the NS3 region of DENV (dsDENV) before infection by feeding. This resulted in abundant production of DENV-derived siRNAs and efficient control of viral replication in the midgut (Fig. 3c-e). Overall, our data indicate that silencing triggered DENV infection is mechanistically different from endogenous and

exogenous sources of dsRNA. We observed production of DENV-derived siRNAs in the midgut even before they were detected in the carcass of orally infected mosquitoes indicating that any defect in antiviral RNAi is downstream of small RNA biogenesis (Fig. 3f).

Our results suggest that siRNAs directly produced from a viral substrate are not functional silencing in the midgut, in contrast to exo- and endo-siRNAs. These results imply that the mosquito siRNA pathway discriminates dsRNAs from viral origin as observed in *Drosophila*[14] and *Caenorhabditis elegans*[15]. Small dsRBPs often regulate different steps of RNA silencing[17,19-21] and allow functional specialization without requiring significant changes in core components of the siRNA pathway[14]. In *Drosophila*, two dsRNA binding proteins (dsRBPs), Loquacius and r2d2, regulate biogenesis and loading of siRNAs[14,16,17]. Loqs-PD is encoded by an isoform of the *loquacious* gene and is required for silencing of endogenous and exogenous sources of dsRNA but not viruses. The Loqs-PD isoform appeared recently in the *Drosophila* lineage[18]. In *A. aegypti*, Loqs-PA encoded by a different isoform of *loquacious* is required for the biogenesis of siRNAs but it does not discriminate viral and endogenous sources of dsRNA[18]. We analyzed the genome of *A. aegypti* to find genes encoding other dsRBPs and identified an uncharacterized gene, *AAEL013721*. Phylogenetic analysis and domain organization indicated that this putative dsRBP is a paralog of both *r2d2* and *loquacious*, more closely related to the latter (Fig. 4a). Hereafter we refer to *AAEL013721* as *loqs2*. The *loqs2* gene is found in the genomes of *A. aegypti* and *A. albopictus* but not in other mosquitoes such as *Culex* and *Anopheles* (Fig. 4a). The *loqs2* gene is widely expressed in most organs from *A. aegypti* but not in the midgut (Fig. 3a). In order to address the contribution of *loqs2* to antiviral defense during systemic infection, we silenced its expression before direct systemic injection of DENV. Mosquitoes treated with dsRNA targeting *loqs2* (dsLoqs2) showed significantly increased levels of DENV RNA (Fig. 4b). These results show that Loqs2 is required to control systemic viral infection. Because *loqs2* is not expressed in the midgut, we hypothesized that it is the missing cofactor for antiviral RNAi in this tissue. We

150 next generated transgenic mosquitoes expressing *loqs2* under the control of the
151 *carboxypeptidase* (*CP*) gene that directs midgut expression in response to blood feeding[22] (Fig.
152 4c-e). The transgene was inherited at normal Mendelian ratios and mosquitoes showed no visible
153 abnormalities. When exposed to an infectious blood meal, transgenic mosquitoes showed
154 significantly reduced DENV load in the midgut at 4 and 8 dpf (Fig. 4f,g). This likely resulted in
155 lower virus dissemination since the prevalence of infection was significantly reduced in the
156 carcass of transgenic mosquitoes (Fig. 4h,i). To identify potential protein partners, we
157 immunoprecipitated Loqs2 from Aag2 cells and performed mass spectrometry analysis (Fig. 4j).
158 A total of 79 proteins were significantly enriched in the Loqs2 immunoprecipitation compared to
159 the control (Supplementary Table 1). Loqs and r2d2, the two dsRBPs involved in siRNA
160 biogenesis and loading, were among the 4 most significant hits (Fig. 4j). These results suggest
161 that Loqs2 works together with Loqs and r2d2 to allow the siRNA pathway to control viral infection.
162 In order to evaluate whether Loqs2 was broadly required for the control of arboviruses, we
163 analyzed ZIKV infection in mosquitoes. The prevalence of disseminated ZIKV infection in the
164 carcass after an infectious blood meal was low at 4 dpf and increased by 8 dpf (Supplementary
165 Fig. 3a,b). In contrast, mosquitoes treated with dsRNA to silence *loqs2* (dsLoqs2) had significantly
166 increased ZIKV replication and dissemination to the carcass at 4 dpf compared to control
167 mosquitoes (Supplementary Fig. 3c,d). These data suggest that Loqs2 is also important to control
168 ZIKV dissemination.
169
170 In summary, our results reveal that the siRNA pathway controls DENV and ZIKV infection during
171 systemic dissemination but not in the midgut. Interestingly, control of O'nyong-nyong virus in the
172 midgut of *Anopheles* mosquitoes also seems to be independent on the siRNA pathway[23]. This
173 tissue-specific defect suggests the existence of specialization in the mosquito siRNA pathway
174 since silencing triggered by exogenous and endogenous dsRNAs appears fully operational in the
175 midgut. Functional specialization of the siRNA pathway in response to viruses has been reported

176 in different organisms and might be required for optimizing the antiviral defense[14,24-26]. We
177 identified an *Aedes* specific dsRBP, Loqs2*,* that is required for systemic control of DENV likely by
178 regulating the antiviral arm of the siRNA pathway. Further studies are necessary to determine
179 how Loqs2 would specifically affect antiviral silencing but not the siRNA pathway triggered by
180 endogenous and exogenous sources of dsRNA. It is also unclear why *loqs2* is not expressed in
181 the midgut, unlike other components of the siRNA pathway. The Loqs-PD isoform in *Drosophila*
182 and *loqs2* in *Aedes* mosquitoes evolved independently, suggesting there is selective pressure to
183 separate the antiviral arm of the siRNA pathway. Finally, it is interesting to speculate whether the
184 specialization of the siRNA pathway we described in *Aedes* mosquitoes is connected to their
185 exquisite vector competence for viruses.
186

Methods

Ethics statement. All procedures involving vertebrate animals were approved by the ethical review committee of the Universidade Federal de Minas Gerais (CEUA 337/2016 to J.T.M.). Blood for membrane feeding was obtained from a blood bank in Belo Horizonte (Brazil) accordingly to protocol approved by the Committee for Ethics in Research (CEP)/FIOCRUZ (License CEP 732.621 to L.A.M.).

Virus propagation. Viral isolates of DENV4 (H241 strain), DENV1[27] and ZIKV (PE243/2015)[28] were propagated in C6/36 *A. albopictus* cells maintained on L15 medium supplemented with 5% FBS (fetal bovine serum), penicillin, streptomycin and gentamycin as described[29]. Briefly, cells were seeded to 70% confluency and infected at a multiplicity of infection (MOI) of 0.01. Culture was maintained for 9 days at 28˚C and supernatant was collected apart from cells, that were lysed by repeated freezing and thawing for releasing virus particles and mixed to supernatant. After clarifying the supernatant by centrifugation, virus stocks were kept at -80˚C prior to use. Mock-infected supernatants used as controls were prepared under same procedure without virus infection.

Gene-silencing. RNA transcription was performed utilizing T7/SP6 Megascript® Kits (Ambion™) following manufacturer instructions. Briefly, a template DNA containing both promoter sequences were obtained by RT-qPCR for dsAGO2 and dsDENV; by PCR amplification from a pGL3-Basic plasmid (Promega Inc.) containing the Firefly luciferase sequence for dsFLUC; and by PCR amplification from plasmid pDSAG (Addgene #62289) for dsGFP. Primer sequences are available in Supplementary Table 2. Adult 4 days old females were intrathoracically injected with 69 nL of a double-stranded RNA (dsRNA) solution (7.2 µg/µL) diluted in annealing buffer (20mM Tris-HCl pH 7.5, 100mM NaCl) using a nano-injector Nanoject II™ (Drummond Scientific Company). Mosquitoes were allowed to recover for 48 hours prior to feeding or virus injection.

Mosquito strains. For initial experiments of natural resistance, we also utilized F1 and F2 generations of wild *A. aegypti* mosquitoes raised in the laboratory from eggs collected in three neighborhoods of Rio de Janeiro (Humaita, Tubiacanga and Belford Roxo), in southeastern Brazil. For silencing experiments, we utilized mosquitoes from the Red-eye strain[30]. For the generation of transgenic individuals, wild-type mosquitoes without docking sites were selected from strain 12 of BEI Resources (NIAID, NIH: *A. aegypti*, Strain Line 12, MRA-863, contributed by Paul Eggleston). Wild and laboratory mosquito colonies show similar prevalence of infection and viral loads after feeding on a DENV-infected blood meal.

Mosquito rearing and infections. *A. aegypti* mosquitoes were maintained in an incubator at 28°C and 70-80% relative humidity, in a 12:12 hour light:dark photoperiod, and 10% sucrose solution *ad libitum*. For infections by membrane feeding, 5-6 day old adult females were starved for 24h and fed with a mixture of blood and virus supernatant containing 10^7 PFU/mL of DENV4 utilizing a glass artificial feeding system covered with pig intestine membrane. For mosquito infections utilizing mice, we used previously described models for flavivirus infections in IFN deficient animals[31]. AG129 and A129 mice were injected intraperitoneally with 10^6 PFU of DENV1 and ZIKV, respectively. Infected mice were anaesthetized 3 days post infection (peak of viremia) using ketamine/xylazine (80/8 mg per kg) and placed on top of the netting-covered containers with 5-6 day old adult mosquito females. Mosquitoes were allowed to feed on mice for 1h. After blood feeding, fully engorged females were selected and harvested individually for RNA extraction or dissection at different time points. Mosquitoes infected by injection were anesthetized with carbon dioxide and kept on ice during the whole procedure. Virus stocks were diluted with L15 medium and injections were performed as previously described for gene-silencing procedure. Each individual mosquito was injected with 160 PFU of DENV unless stated otherwise. Mosquitoes were harvested at different days post injection for RNA extraction. Tissues or mosquitoes were grounded in TRIzol® (Invitrogen™) using glass beads as previously described[9].

Total RNA was extracted from individual mosquitoes or individual tissues according to manufacturer's protocol.

RT-qPCR. 200 ng of total RNA extracted from individual insects or individual tissues were reverse transcribed using MMLV reverse transcriptase. cDNA was subjected to quantitative polymerase chain reaction (qPCR) utilizing the kit Power SYBR® Green Master Mix (Applied Biosystems) following manufacturer instructions. Specific primers are listed on Supplementary Table 2.

Strand-specific RT-PCR. Total RNA was used in each cDNA reaction, being made 4 reactions at a time: DENV cDNAs of both polarities were reverse transcribed from primers containing a 5' tag sequence[32]. Mosquito mRNAs were reverse transcribed using oligo $(dT)_{18}$, and negative control reactions were carried out without addition of primers. First, a mixture of total RNA (200 ng), dNTP (10 nmol each) and primers (2 fmol for specific oligos or 100 fmol for oligo $(dT)_{18}$) was incubated for 5 min at 70˚C and for 2 min at 52˚C. Samples were immediately incubated on ice and a reaction mix containing Superscript™ III (200 U) (Invitrogen™), First-Strand Buffer (1X) and DTT (100 mmol) was added. Samples were incubated for 55 min at 52˚C, followed by an incubation of 15 min at 70˚C for enzyme inactivation. Unincorporated primers were digested by a 30 min incubation at 37˚C with exonuclease I (50 U) (New England Biolabs). 2 µL of each cDNA was used for PCR amplification with Platinum® Taq DNA polymerase (Invitrogen™) and specific primers (Supplementary Table 2) following standard recommendations from the manufacturer.

Indirect immunofluorescence assays (IFA). Mosquitoes were anesthetized with carbon monoxide and kept in ice-cold PBS solution (13 mM NaCl, 0.7 mM Na_2HPO_4, 1 mM NaH_2PO_4 at pH 7.2) during dissection process. Midguts were fixed in 4% paraformaldehyde for 30 min at 25°C, washed with PBS twice for 5 min and incubated for 1 h in blocking solution PBST (1X PBS + 1% Bovine Serum Albumin + 0.1 % Triton X-100) with rocking at 25°C. Flavivirus E protein was detected using the 4G2 monoclonal antibody (ATCC: HB-112, used at 1:50 in PBST) for 1h at 25°C . Midguts were washed 5 times with PBST (5 min each) and incubated for 1 h with constant rocking at 25°C with goat anti-mouse IgG antibody conjugated to Alexa 488 (Molecular Probes™,

1:500), Hoechst 33342 (Trihydrochloride, Trihydrate - Molecular Probes™, 1:1000) and Phalloidin-Rhodamine (Molecular Probes™, 1:500). Subsequently, midguts were washed twice with PBST with constant rocking at 25°C for 90 min, rinsed with PBS and placed onto slides. Images were obtained with Apotome.2 microscope (Zeiss). Area measurements of infection foci were performed using ImageJ v1.51e (https://imagej.nih.gov/ij/).

Small RNA library construction and bioinformatic analyses. Two strategies for library construction were used as indicated in Supplementary Table 2. (i) Small RNAs were selected by size (18–30 nt) on a denaturing PAGE before being used for construction of libraries as previously described[33]. In this case, RNA adaptors containing 4 random nucleotides at 5' and 3' extremities were used to prevent cloning bias as described before[9,34]. (ii) Total RNA was used as input for library preparation utilizing the TruSeq® Small RNA Library Prep Kit (Illumina®). Both strategies yielded similar results. After sequencing, raw sequenced reads from small RNA libraries were submitted to adaptor trimming using cutadapt[35] v1.12, discarding sequences smaller than 18 nt. Remaining sequences were mapped to *A. aegypti* reference genome (AaeL3.3), DENV genome and *A. aegypti* TEfam transposable elements (https://tefam.biochem.vt.edu/tefam/) using Bowtie[36] v1.1.2 allowing no mismatches and discarding reads mapping on multiple regions. Size profiles of small RNAs matching DENV genome and 5' nt frequency were calculated using in-house Perl v5.16.3, BioPerl library v1.6.924 and R v3.3.1 scripts. Plots were made in R using ggplot2 v2.2.0 package. Transcriptome analysis of public data was performed using raw reads as input for STAR[37] v2.5.2b, following normalization by RSEM[38] v1.2.31 and edgeR[39] v3.16.5.

Phylogenetic analysis. Protein sequences containing DS_RBD (Double-stranded RNA-binding domain), InterPRO accession IPR014720, were retrieved from Flybase, VectorBase and WormBase, respectively (gene accession identifiers: *D. melanogaster* - CG7138 (*r2d2*), CG6866 (*loquacious*); *A. aegypti* - AAEL011753 (*r2d2*), AAEL008687 (*loquacious*), AAEL013721 (*loqs2*); *A. albopictus* - AALF015406 (r2d2), AALF018531 (*loquacious*), AALF016290 (*loqs2*); *C. quinquefasciatus* - CPIJ011746 (r2d2), CPIJ004832 (*loquacious*); *A. gambiae* - AGAP009887

(*r2d2*), AGAP009781 (*loquacious*); *C. elegans* – T20G5.11 (*rde-4*)). Full open reading frames were aligned using ClustalO[40] v1.2.4 with standard parameters. Phylogenetic tree was constructed using FigTree v1.4.3 (http://tree.bio.ed.ac.uk/software/figtree).

Plasmid constructions. Plasmids were prepared using GoldenGate cloning[41-43]. Details for main plasmids are described on Supplementary Table 3 and sequences are provided in Supplementary Information. Briefly, DNA fragments were PCR-amplified using Phusion High-Fidelity DNA polymerase (Thermo Scientific™) with oligos described in Supplementary Table 2. PCR products for GoldenGate cloning were designed to have BsaI sites in their extremities. All PCR products were cloned into a modified pBluescriptII KS(+) (Addgene #62540) lacking BsaI restriction site in an one-step digestion/ligation using FastDigest™ SmaI or FastDigest™ EcoRV (Thermo Scientific™) and T4 DNA-ligase (Invitrogen™) with 10mM ATP. Final plasmid assembly by GoldenGate cloning was conducted as described[43]. Successful cloning was confirmed by Sanger sequencing (GATC Biotech, Germany).

Mosquito Transgenesis. Embryo microinjection was performed with small modifications as previously described[43-45]. Briefly, freshly laid eggs were parallelly aligned against the internal side of a [shaped nitrocellulose membrane kept wet with an overlaying filter paper soaked in demineralized water. Aligned eggs rested in a humid chamber for 30-60 minutes after alignment, until the eggs turned dark-grey. A plasmid mix containing 100 ng/µL of transposase helper-plasmid and 400 ng/µL of plasmids carrying *piggyBac*-flanked cassettes (described in Supplementary table 3) were diluted in 0.5X PBS and were injected at the embryo posterior-pole under a Nikon Eclipse TE2000-S inverted microscope using a Femtojet injector (Eppendorf) and a TransferMan NK2 micromanipulator. Before being dried, microinjected eggs were allowed to rest for 2 days placed diagonally in a container with 1-cm-deep water. The filter-paper had direct contact with water that maintained the eggs wet by capillarity. Surviving eggs were hatched under vacuum and larvae showing transient expression of fluorescent markers were kept for further crossing to an excess of wild-type mosquitoes. Single transgenic females were crossed to wild-

type males to start isofamilies. Infection experiments performed with 3 independent transgenic lines carrying single insertions of the transgene showed similar phenotypes.

Immunoprecipitation of Loqs2. *A. aegypti* Aag2 cells were grown at 25˚C in Schneider medium supplemented with 10% FBS, 1% penicillin-streptomycin and 1% GlutaMAX™ (Gibco). Prior transfection, 3 x 10^6 cells were seeded in each well of a 6 wells plates and transfected with 800 ng of plasmid DNA using Effectene Reagent (QUIAGEN), following manufacturer instructions. Media was replaced 18 h after transfection and cells were allowed to grow for 4 days. Plasmid sequences are described in Supplementary Table 3. Cells were washed and harvested in ice-cold 1X PBS, pelleted by centrifugation at 4˚C and Lysis buffer (30 mM HEPES KOH pH 7.5, 50 mM NaCl, 2 mM $Mg(OAC)_2$, 1% NP40 and Roche protease inhibitor cocktail) was added. Flag-Loqs2 and Flag-eGFP proteins were immunoprecipitated using magnetic microparticles coated with a monoclonal anti-Flag antibody (μMACS magnetic microbeads - MACS purification system, Miltenyi Biotech) according to the manufacturer's instructions and as previously described[46]. Flag-eGFP was used as a negative control. Immunoprecipitation experiments were carried out in triplicates.

Mass spectrometry analysis. Eluted proteins were digested with sequencing-grade trypsin (Promega) and analyzed by nanoLC-MS/MS on a TripleTOF 5600 mass spectrometer (Sciex, USA) coupled to nanoLC-ultra-2D-plus liquid chromatography (Eksigent, Sciex Separations, USA) as described previously[47]. Data were searched against the UniProtKB database (*Aedes aegypti*, taxon 7159, release 2018_03, 24.927 sequences) with a decoy strategy. Peptides were identified with Mascot algorithm[48] (version 2.5, Matrix Science, London, UK) and data were further imported into Proline 1.4 software (http://proline.profiproteomics.fr). Proteins were validated on Mascot pretty rank equal to 1, and 1% FDR on both peptide spectrum matches (PSM score) and protein sets (Protein Set score). The total number of MS/MS fragmentation spectra was used to quantify each protein from at least three independent biological replicates. This spectral count was submitted to a negative-binomial test using an edgeR[39] GLM regression through R v3.2.5.

For each identified protein, an adjusted *p*-value corrected by Benjamini–Hochberg was calculated, as well as a protein fold-change (FC). The results are presented in a Volcano plot using protein $\log_2$ fold changes and their corresponding adjusted $\log_{10}$ *p*-values to highlight upregulated proteins. Data are available via ProteomeXchange with identifier PXD010191.

Statistical analyses. Evaluation of statistical significance was performed using GraphPad Prism™ software or stated otherwise. Viral loads of RT-qPCR positive-only individual mosquito/tissues were log transformed and subjected to Mann-Whitney *U* test. Prevalence of infection was evaluated by Fisher's exact test. The significance of differential gene expression of RNAi components was evaluated using multiple *t*-tests and Holm-Sidak correction method for multiple comparisons. Pearson correlation coefficient was calculated for each group of samples using log-transformed values of normalized viral load (by RpL32 mRNA expression) and normalized siRNA counts (by total number of reads mapping on *A. aegypti* genome).

Data availability

Small RNA libraries from this study were deposited on *Sequence Read Archive* (SRA) at NCBI. Other publicly available RNA-seq datasets were obtained from SRA. Accession numbers and references are described in Supplementary Table 4.

Correspondence and requests for materials should be addressed to J.T.M. (jtm@ufmg.br).

Acknowledgments

We thank Claudia N. D. dos Santos for kindly providing 4G2 monoclonal antibodies. This work was supported with funding from Conselho Nacional de Desenvolvimento Científico e Tecnológico (CNPq), Coordenação de Aperfeiçoamento de Pessoal de Nível Superior (CAPES) and Fundação de Amparo a Pesquisa do Estado de Minas Gerais (FAPEMIG) to J.T.M.; Agence Nationale de la Recherche (ANR-11-ASV3-002), Investissement d'Avenir Programs (ANR-10-LABX-36; ANR-11-EQPX-0022) to J.T.M and J.-L.I.; Inserm, CNRS and the University of Strasbourg to E.M. and J.-L.I.; mass spectrometry instrumentation was funded by University of Strasbourg, IdEx Equipement mi-lourd 2015 to L.K. and P.H.. National and/or international fellowships from CAPES were granted to R.P.O., T.C.I.-T., A.G.A.F., E.R.G.R.A., K.P.R.S., K.P.O., and C.D.O.; national and/or international fellowships from CNPq were granted to I.J.S.F., L.A.M. and J.T.M..

Author contributions

R.P.O. and J.T.M. designed the project. R.P.O., A.G.A.F., T.C.I.-T., I.J.S.F., K.P.R.S., K.P.O., P.H., E.G.A., Y.M.T, M.N.R., T.H.J.F.L., S.C.G.A., J.N.A., S.P. performed experiments. R.P.O., E.R.G.R.A. and L.K. performed bioinformatics analysis. C.D.O., F.D.C., L.A.M and E.M. contributed to mosquito experiments. R.P.O., E.R.G.R.A., J.-L.I. and J.T.M. analyzed the data.

R.P.O., J.-L.I. and J.T.M. wrote the paper. All authors discussed the results and commented on the manuscript.

Competing interests

The authors declare no competing financial interests.

Additional information

Supplementary information is available online. Reprints and permissions information is available online at www.nature.com/reprints.

389 **Figure legends**

390

391 **Figure 1 - Production of DENV-derived siRNAs in infected mosquitoes.** (**a**) Mosquitoes were
392 fed on a blood meal containing 10^7 PFU/mL of DENV and tested individually by RT-qPCR to
393 detect viral RNA levels. After 4 days post feeding (dpf), three different groups were observed:
394 mosquitoes with detectable viral RNA at high or low viral loads (full circles), and individuals with
395 undetected viral load (open circles). Control mosquitoes were fed on a blood meal without virus.
396 The dashed line indicates the lower limit of viral RNA levels detected at 2 dpf. (**b**) Detection of the
397 DENV antigenome as an indication of productive viral replication in pools of mosquitoes from
398 each group. This experiment is representative of three biological replicates. **c-f** Size distribution
399 and 5' base frequency of DENV-derived small RNA sequences from different mosquito groups:
400 (**c**) high viral load, (**d**) low viral load, (**e**) undetected viral load and (**f**) controls. Positive and
401 negative values reflect sequences that matched the sense and antisense strands of the viral
402 genome, respectively. Viral load of each RNA pool is indicated in each plot. (**g**) Mosquitoes were
403 intrathoracically injected with 160 PFU of DENV and tested individually by RT-qPCR to detect the
404 viral RNA. (**h**) Size distribution and 5' base frequency of DENV-derived small RNA sequences
405 from mosquitoes injected with DENV at different times after infection. dpf, days post feeding; dpi,
406 days post injection. In **a** and **g**, numbers of infected individuals over the total number of
407 mosquitoes are indicated above each column. Each dot represents a mosquito. Bars show
408 median and interquartile range. Only mosquitoes with detectable viral load were considered for
409 statistical analyses.

410

411 **Figure 2 – The antiviral siRNA pathway does not control DENV infection in the mosquito**
412 **midgut but inhibits systemic dissemination and replication.** (**a**) Detailed strategy to analyze
413 DENV infection in mosquitoes by measuring viral load by RT-qPCR or detection of envelope (E)
414 protein by immunofluorescence (IFA) microscopy. (**b**) DENV RNA levels and (**c**) prevalence of

415 infection in the midgut of mosquitoes treated with dsAGO2 or dsFLUC at indicated time points
416 after feeding on an DENV-contaminated blood meal. Numbers of infected individuals over the
417 total are indicated above each tested condition. In **c** numbers of infected midguts over the total
418 number analyzed are indicated above each column. Each dot represents a midgut from a single
419 mosquito. (**d**) Number of foci per midgut of DENV infected mosquitoes treated with dsAGO2 or
420 dsFLUC at 3 and 4 days post feeding. n= 13 and n= 15 midguts of dsFLUC or dsAGO2 treated
421 mosquitoes, respectively. (**e**) Size of DENV infected foci in the midgut of mosquitoes treated with
422 dsAGO2 or dsFLUC at 3 and 4 dpf. Error bars represent median and interquartile range. n= 34
423 and n= 31 DENV foci from midguts of dsFLUC or dsAGO2 treated mosquitoes, respectively. Two-
424 tailed Mann-Whitney U test was performed in **b**, **d** and **e**. Two-tailed Fisher's exact test was used
425 in **c**. *ns*, non-significant. (**f**) Prevalence of DENV infection and (**g**) DENV RNA levels in the carcass
426 of mosquitoes treated with dsAGO2 or dsFLUC at indicated time points after feeding on an
427 infectious blood meal. Numbers of infected individuals over the total are indicated above each
428 condition. (**h**) DENV RNA levels in mosquitoes treated with dsAGO2 or dsFLUC and injected
429 intrathoracically with DENV to mimic systemic infection. In **f** and **h**, error bars represent median
430 and interquartile range, statistical significance was determined by two-tailed Mann-Whitney U test.
431 *ns*, non-significant. Numbers of infected carcasses (**f**) or whole mosquitoes (**g**) over the total
432 number tested are indicated above each column where each dot represents an individual sample.
433 Bars show median and interquartile range. In **g,** *p*-values are indicated based on two-tailed
434 Fisher's exact test.
435
436 **Figure 3 – The siRNA pathway triggered by endogenous and exogenous sources of dsRNA**
437 **is functional in the midgut.** (**a**) Expression levels of siRNA pathway components based on
438 individual RNAseq libraries from embryos (em, n=3), adult whole bodies (wb, n=6), brains (br,
439 n=3), salivary glands (sg, n=2), ovaries (ov, n=2) and midguts (mi, n=6). FPKM, fragments per
440 kilobase per million. Bars represent mean and standard deviation. Two-tailed one-way ANOVA

followed by Dunnet's test was applied. *ns*, not significant. (**b**) Transposable element (TE)-derived siRNA levels in the midgut of mosquitoes treated with dsAGO2 or dsFLUC. RPM, reads per million. n=150. Two-tailed paired *t*-test with Holm-Sidak correction method for multiple comparisons was applied. (**c**) Size distribution and 5' base frequency of DENV-derived small RNA sequences in the midgut of mosquitoes injected with dsRNA targeting the NS3 region of DENV genome (dsDENV). The plot on bottom shows the density of siRNAs on the DENV genome. dsRNA target region is indicated by a black bar. (**d**) DENV viral load in the midgut of mosquitoes treated with dsDENV or dsFLUC at 4 dpf. Numbers of infected midguts over the total number tested are indicated above each column. Each dot represents a midgut from a single mosquito. Bars show median and interquartile range. Two-tailed Mann-Whitney U test was applied. (**e**) Prevalence of DENV infection in the midguts from **d**. Two tailed Fisher's exact test was applied.(**f**) Size distribution and 5' base frequency of DENV-derived small RNAs in the midgut or carcasses of mosquitoes with disseminated viral infection. DENV load in each RNA sample is indicated in the plot.

Figure 4 – The *Aedes*-specific dsRBP Loqs2 regulates the antiviral arm of the mosquito siRNA pathway. (**a**) Phylogeny of dsRNA binding proteins (dsRBPs) found in the genomes of *D. melanogaster* (Dm), *Anopheles gambiae* (Ag), *Culex quinquefasciatus* (Cq), *A. aegypti* (Ae), *Aedes albopictus* (Aa) and *C. elegans* (Ce). Domain organization for each dsRBP is indicated. (**b**) Viral RNA levels upon DENV injection in dsLoqs2 treated mosquitoes compared to controls (dsGFP). Numbers of infected whole mosquitoes over the total number tested are indicated above each column. Each dot represents an individual mosquito. Bars show median and interquartile range. Two-tailed Mann-Whitney U test was applied. (**c**) Construct for inducible expression of *loqs2* in *A. aegypti* under the control of the *carboxypeptidase (CP)* promoter. (**d**) Fluorescent marker expression in transgenic larvae. Results are representative of images observed with at least three independent transgenic lines. (**e**) *loqs2* mRNA levels in the carcass and midgut of

control and transgenic mosquitoes upon blood feeding. Bars represent mean and standard deviation. Number of independent biological samples is indicated in the figure. ND, not detected. (**f**) Viral RNA levels and (**g**) prevalence of infection in the midgut of control and transgenic mosquitoes at indicated time points after feeding on DENV infected mice. (**h**) Viral RNA levels and (**i**) prevalence of infection in the carcass of control and transgenic mosquitoes at indicated time points after feeding on DENV infected mice. In **f** and **h**, numbers of infected midguts (**f**) or carcasses (**h**) over the total number tested are indicated above each column. Each dot represents an individual midgut (**f**) or carcass (**h**). Bars show median and interquartile range. Two-tailed Mann-Whitney U test was applied. In **g** and **i**, two-tailed Fisher's exact test was applied. *ns*, non-significant. (**j**) Proteins enriched in immunoprecipitates of Loqs2 (right side of the graph) compared to the control (GFP, left side of the graph). Spectral counts were submitted to a negative-binomial test using GLM regression. *p*-values were corrected using the Benjamini–Hochberg method. n=3 independent samples.

References

1 Guzman, M. G., Gubler, D. J., Izquierdo, A., Martinez, E. & Halstead, S. B. Dengue infection. *Nature reviews. Disease primers* **2**, 16055 (2016).

2 Sanchez-Vargas, I. *et al.* Dengue virus type 2 infections of Aedes aegypti are modulated by the mosquito's RNA interference pathway. *PLoS Pathog* **5**, e1000299 (2009).

3 Khoo, C. C. H., Piper, J., Sanchez-Vargas, I., Olson, K. E. & Franz, A. W. E. The RNA interference pathway affects midgut infection- and escape barriers for Sindbis virus in Aedes aegypti. *BMC Microbiol* **10**, 130 (2010).

4 Franz, A. W. *et al.* Engineering RNA interference-based resistance to dengue virus type 2 in genetically modified Aedes aegypti. *Proc Natl Acad Sci U S A* **103**, 4198-4203 (2006).

5 Campbell, C. L. *et al.* Aedes aegypti uses RNA interference in defense against Sindbis virus infection. *BMC Microbiol* **8**, 47 (2008).

6 Hess, A. M. *et al.* Small RNA profiling of Dengue virus-mosquito interactions implicates the PIWI RNA pathway in anti-viral defense. *BMC Microbiol* **11**, 45 (2011).

7 Miesen, P., Ivens, A., Buck, A. H. & van Rij, R. P. Small RNA Profiling in Dengue Virus 2-Infected Aedes Mosquito Cells Reveals Viral piRNAs and Novel Host miRNAs. *PLoS Negl Trop Dis* **10**, e0004452-0004422 (2016).

8 Villalon, J. M., Ghosh, A. & Jacobs-Lorena, M. The peritrophic matrix limits the rate of digestion in adult Anopheles stephensi and Aedes aegypti mosquitoes. *Journal of insect physiology* **49**, 891-895 (2003).

9 Aguiar, E. R. G. R., Olmo, R. P. & Marques, J. T. Virus-derived small RNAs: molecular footprints of host-pathogen interactions. *Wiley Interdiscip Rev RNA* (2016).

10 Richardson, J., Molina-Cruz, A., Salazar, M. I. & Black, W. t. Quantitative analysis of dengue-2 virus RNA during the extrinsic incubation period in individual Aedes aegypti. *Am J Trop Med Hyg* **74**, 132-141 (2006).

11 Salazar, M. I., Richardson, J. H., Sánchez-Vargas, I., Olson, K. E. & Beaty, B. J. Dengue virus type 2: replication and tropisms in orally infected Aedes aegypti mosquitoes. *BMC microbiology* **7**, 9 (2007).

12 Carthew, R. W. & Sontheimer, E. J. Origins and Mechanisms of miRNAs and siRNAs. *Cell* **136**, 642-655 (2009).

13 Ghildiyal, M. *et al.* Endogenous siRNAs Derived from Transposons and mRNAs in Drosophila Somatic Cells. *Science* **320**, 1077-1081 (2008).

14 Marques, J. T. *et al.* Functional specialization of the small interfering RNA pathway in response to virus infection. *PLoS Pathog* **9**, e1003579 (2013).

15 Ashe, A. *et al.* A deletion polymorphism in the Caenorhabditis elegans RIG-I homolog disables viral RNA dicing and antiviral immunity. *eLIFE* **2**, e00994 (2013).

16 Hartig, J. V., Esslinger, S., Böttcher, R., Saito, K. & Förstemann, K. Endo-siRNAs depend on a new isoform of loquacious and target artificially introduced, high-copy sequences. *EMBO J* **28**, 2932-2944 (2009).

17 Hartig, J. V. & Förstemann, K. Loqs-PD and R2D2 define independent pathways for RISC generation in Drosophila. *Nucleic Acids Res* **39**, 3836-3851 (2011).

18 Haac, M. E., Anderson, M. A., Eggleston, H., Myles, K. M. & Adelman, Z. N. The hub protein loquacious connects the microRNA and short interfering RNA pathways in mosquitoes. *Nucleic Acids Res* **43**, 3688-3700 (2015).

19 Marques, J. T. *et al.* Loqs and R2D2 act sequentially in the siRNA pathway in Drosophila. *Nat Struct Mol Biol* **17**, 24-30 (2010).

20 Tabara, H., Yigit, E., Siomi, H. & Mello, C. C. The dsRNA binding protein RDE-4 interacts with RDE-1, DCR-1, and a DExH-box helicase to direct RNAi in C. elegans. *Cell* **109**, 861-871 (2002).

21 Parrish, S. & Fire, A. Distinct roles for RDE-1 and RDE-4 during RNA interference in Caenorhabditis elegans. *RNA* **7**, 1397-1402 (2001).

22 Edwards, M. J. *et al.* Characterization of a carboxypeptidase A gene from the mosquito, Aedes aegypti. *Insect Mol Biol* **9**, 33-38 (2000).

23 Carissimo, G. *et al.* Antiviral immunity of Anopheles gambiae is highly compartmentalized, with distinct roles for RNA interference and gut microbiota. *Proc Natl Acad Sci U S A* **112**, E176-185 (2015).

24 Sarkies, P. *et al.* Ancient and novel small RNA pathways compensate for the loss of piRNAs in multiple independent nematode lineages. *PLoS Biol* **13**, e1002061 (2015).

25 Maillard, P. V. *et al.* Antiviral RNA interference in mammalian cells. *Science* **342**, 235-238 (2013).

26 Li, Y., Lu, J., Han, Y., Fan, X. & Ding, S. W. RNA interference functions as an antiviral immunity mechanism in mammals. *Science* **342**, 231-234 (2013).

27 Pereira, T. N., Rocha, M. N., Sucupira, P. H. F., Carvalho, F. D. & Moreira, L. A. Wolbachia significantly impacts the vector competence of Aedes aegypti for Mayaro virus. *Sci Rep* **8**, 6889 (2018).

28 Donald, C. L. *et al.* Full Genome Sequence and sfRNA Interferon Antagonist Activity of Zika Virus from Recife, Brazil. *PLoS Negl Trop Dis* **10**, e0005048 (2016).

29 Sedda, L. *et al.* The spatial and temporal scales of local dengue virus transmission in natural settings: a retrospective analysis. *Parasites & vectors* **11**, 79 (2018).

30 Barletta, A. B. *et al.* Microbiota activates IMD pathway and limits Sindbis infection in Aedes aegypti. *Parasites & vectors* **10**, 103 (2017).

31 Tan, G. K. *et al.* A non mouse-adapted dengue virus strain as a new model of severe dengue infection in AG129 mice. *PLoS Negl Trop Dis* **4**, e672 (2010).

32 Lanford, R. E., Sureau, C., Jacob, J. R., White, R. & Fuerst, T. R. Demonstration of in vitro infection of chimpanzee hepatocytes with hepatitis C virus using strand-specific RT/PCR. *Virology* **202**, 606-614 (1994).

33 Pfeffer, S. *et al.* Identification of virus-encoded microRNAs. *Science* **304**, 734-736 (2004).

34 Jayaprakash, A. D., Jabado, O., Brown, B. D. & Sachidanandam, R. Identification and remediation of biases in the activity of RNA ligases in small-RNA deep sequencing. *Nucleic Acids Res* **39**, e141 (2011).

35 Martin, M. Cutadapt removes adapter sequences from high-throughput sequencing reads. *EMBnet.journal* **17** (2011).

36 Langmead, B., Trapnell, C., Pop, M. & Salzberg, S. L. Ultrafast and memory-efficient alignment of short DNA sequences to the human genome. *Genome Biol* **10**, R25 (2009).

37 Dobin, A. *et al.* STAR: ultrafast universal RNA-seq aligner. *Bioinformatics* **29**, 15-21 (2013).

38 Li, B. & Dewey, C. N. RSEM: accurate transcript quantification from RNA-Seq data with or without a reference genome. *BMC Bioinformatics* **12**, 323 (2011).

39 Robinson, M. D., McCarthy, D. J. & Smyth, G. K. edgeR: a Bioconductor package for differential expression analysis of digital gene expression data. *Bioinformatics* **26**, 139-140 (2010).

40 Sievers, F. *et al.* Fast, scalable generation of high-quality protein multiple sequence alignments using Clustal Omega. *Mol Syst Biol* **7**, 539 (2011).

41 Engler, C. & Marillonnet, S. Combinatorial DNA assembly using Golden Gate cloning. *Methods Mol Biol* **1073**, 141-156 (2013).

42 Geissler, R. *et al.* Transcriptional activators of human genes with programmable DNA-specificity. *PLoS One* **6**, e19509 (2011).

43 Volohonsky, G. *et al.* Tools for Anopheles gambiae Transgenesis. *G3 (Bethesda)* **5**, 1151-1163 (2015).

44 Jasinskiene, N., Juhn, J. & James, A. A. Microinjection of A. aegypti embryos to obtain transgenic mosquitoes. *J Vis Exp*, 219 (2007).

45 Morris, A. C., Eggleston, P. & Crampton, J. M. Genetic transformation of the mosquito Aedes aegypti by micro-injection of DNA. *Med Vet Entomol* **3**, 1-7 (1989).

584 46 Stoetzel, C. *et al.* A mutation in VPS15 (PIK3R4) causes a ciliopathy and affects IFT20
585 release from the cis-Golgi. *Nat Commun* **7**, 13586 (2016).
586 47 Chicher, J. *et al.* Purification of mRNA-programmed translation initiation complexes
587 suitable for mass spectrometry analysis. *Proteomics* **15**, 2417-2425 (2015).
588 48 Perkins, D. N., Pappin, D. J. C., Creasy, D. M. & Cottrell, J. S. Probability-based protein
589 identification by searching sequence databases using mass spectrometry data.
590 *Electrophoresis* **20**, 3551-3567 (1999).
591

Figure 1

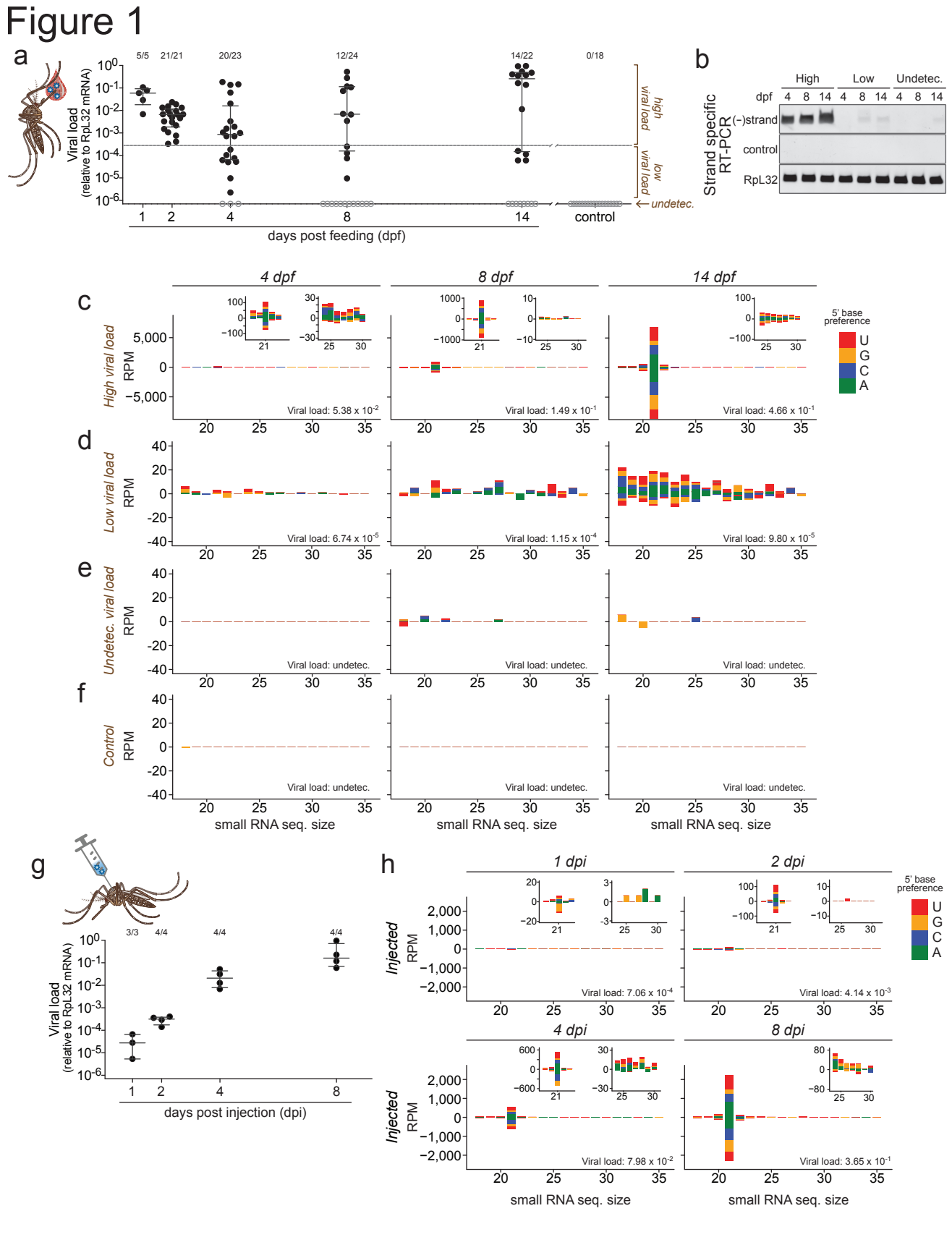
a
5/5
21/21
20/23
12/24
14/22
0/18
Viral load (relative to RpL32 mRNA)
high viral load
low viral load
undetec.
days post feeding (dpf)
control
b
High
Low
Undetec.
dpf
Strand specific RT-PCR
(−)strand
control
RpL32
c
4 dpf
8 dpf
14 dpf
High viral load
RPM
5' base preference
U
G
C
A
Viral load: 5.38 x 10-2
Viral load: 1.49 x 10-1
Viral load: 4.66 x 10-1
d
Low viral load
Viral load: 6.74 x 10-5
Viral load: 1.15 x 10-4
Viral load: 9.80 x 10-5
e
Undetec. viral load
Viral load: undetec.
f
Control
small RNA seq. size
g
3/3
4/4
4/4
4/4
days post injection (dpi)
h
1 dpi
2 dpi
4 dpi
8 dpi
Injected
Viral load: 7.06 x 10-4
Viral load: 4.14 x 10-3
Viral load: 7.98 x 10-2
Viral load: 3.65 x 10-1

Figure 2

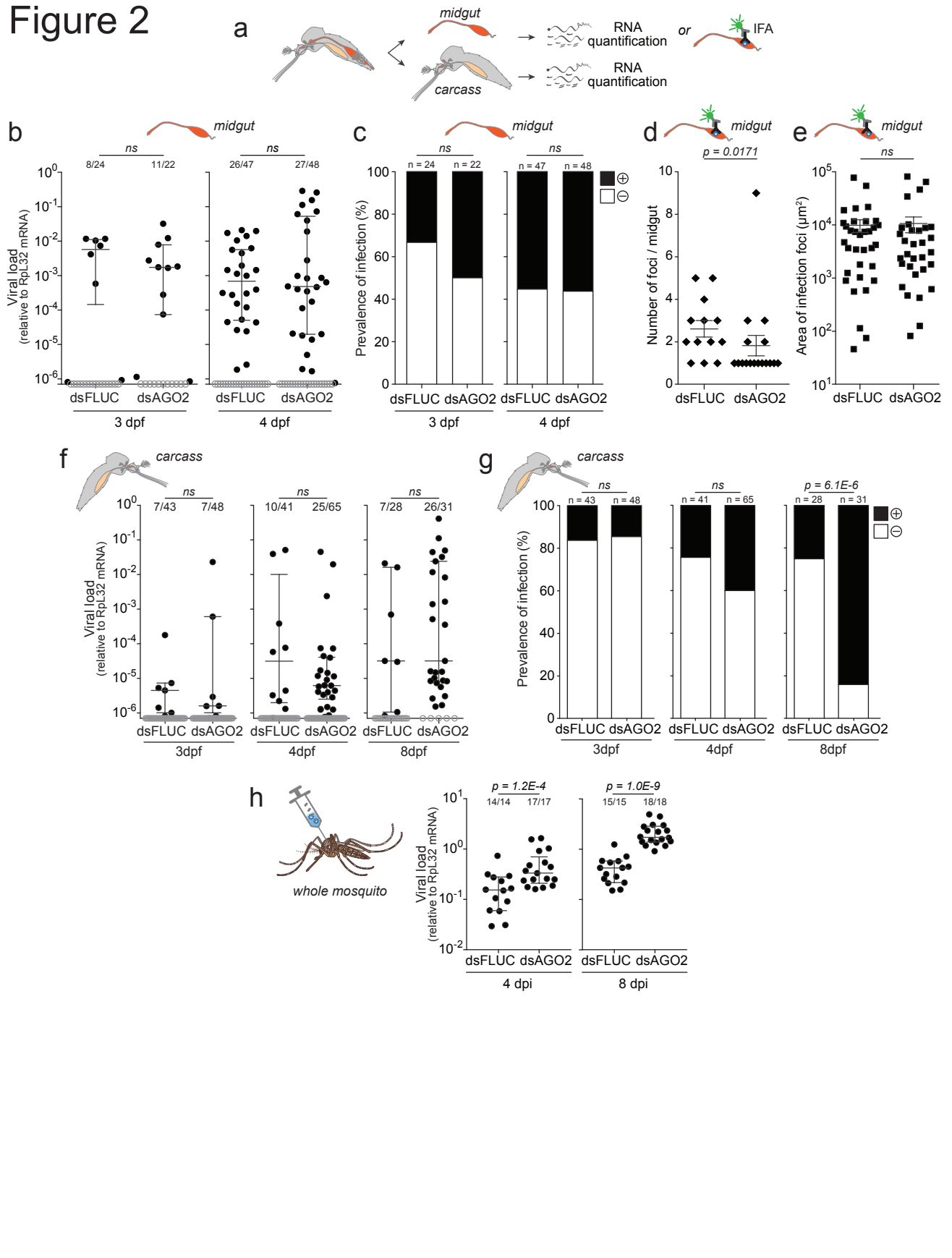
a
midgut
carcass
RNA quantification
or
IFA
RNA quantification
b
midgut
ns
8/24
11/22
ns
26/47
27/48
Viral load (relative to RpL32 mRNA)
dsFLUC
dsAGO2
3 dpf
4 dpf
c
midgut
ns
n = 24
n = 22
ns
n = 47
n = 48
Prevalence of infection (%)
dsFLUC dsAGO2 dsFLUC dsAGO2
3 dpf
4 dpf
d
midgut
p = 0.0171
Number of foci / midgut
dsFLUC
dsAGO2
e
midgut
ns
Area of infection foci (µm²)
dsFLUC
dsAGO2
f
carcass
ns
7/43
7/48
ns
10/41
25/65
ns
7/28
26/31
Viral load (relative to RpL32 mRNA)
dsFLUC dsAGO2
3dpf
4dpf
8dpf
g
carcass
ns
n = 43
n = 48
ns
n = 41
n = 65
p = 6.1E-6
n = 28
n = 31
Prevalence of infection (%)
dsFLUC dsAGO2
3dpf
4dpf
8dpf
h
whole mosquito
p = 1.2E-4
14/14
17/17
p = 1.0E-9
15/15
18/18
Viral load (relative to RpL32 mRNA)
dsFLUC dsAGO2
4 dpi
8 dpi

Figure 3

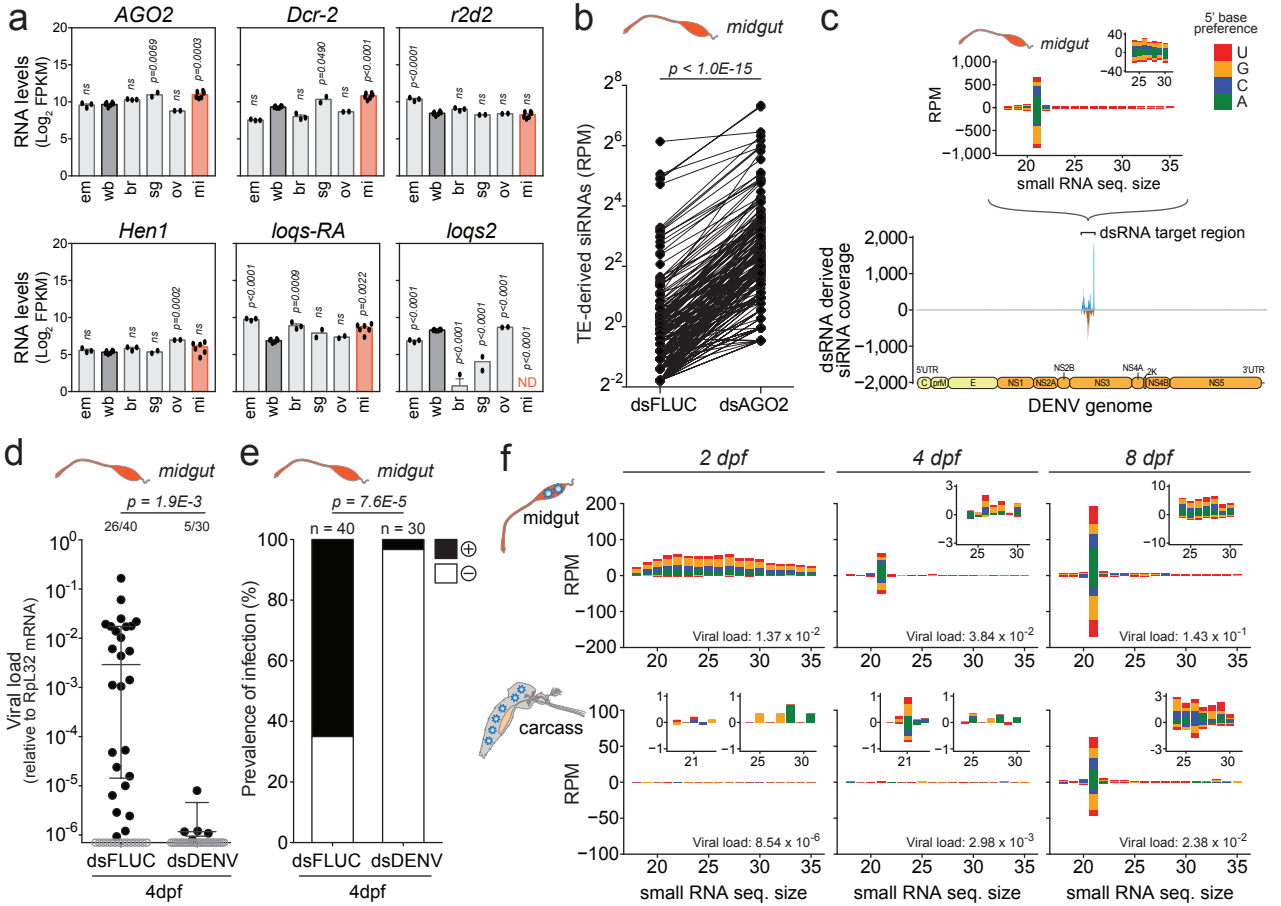
a
AGO2
Dcr-2
r2d2
Hen1
loqs-RA
loqs2
RNA levels (Log2 FPKM)
em wb br sg ov mi
b
midgut
p < 1.0E-15
TE-derived siRNAs (RPM)
dsFLUC dsAGO2
c
midgut
5' base preference
U G C A
RPM
small RNA seq. size
dsRNA target region
dsRNA derived siRNA coverage
5'UTR C prM E NS1 NS2A NS2B NS3 NS4A 2K NS4B NS5 3'UTR
DENV genome
d
midgut
p = 1.9E-3
26/40 5/30
Viral load (relative to RpL32 mRNA)
dsFLUC dsDENV
4dpf
e
midgut
p = 7.6E-5
n = 40 n = 30
Prevalence of infection (%)
dsFLUC dsDENV
4dpf
f
2 dpf
4 dpf
8 dpf
midgut
carcass
RPM
Viral load: 1.37 x 10-2
Viral load: 3.84 x 10-2
Viral load: 1.43 x 10-1
Viral load: 8.54 x 10-6
Viral load: 2.98 x 10-3
Viral load: 2.38 x 10-2
small RNA seq. size

Figure 4

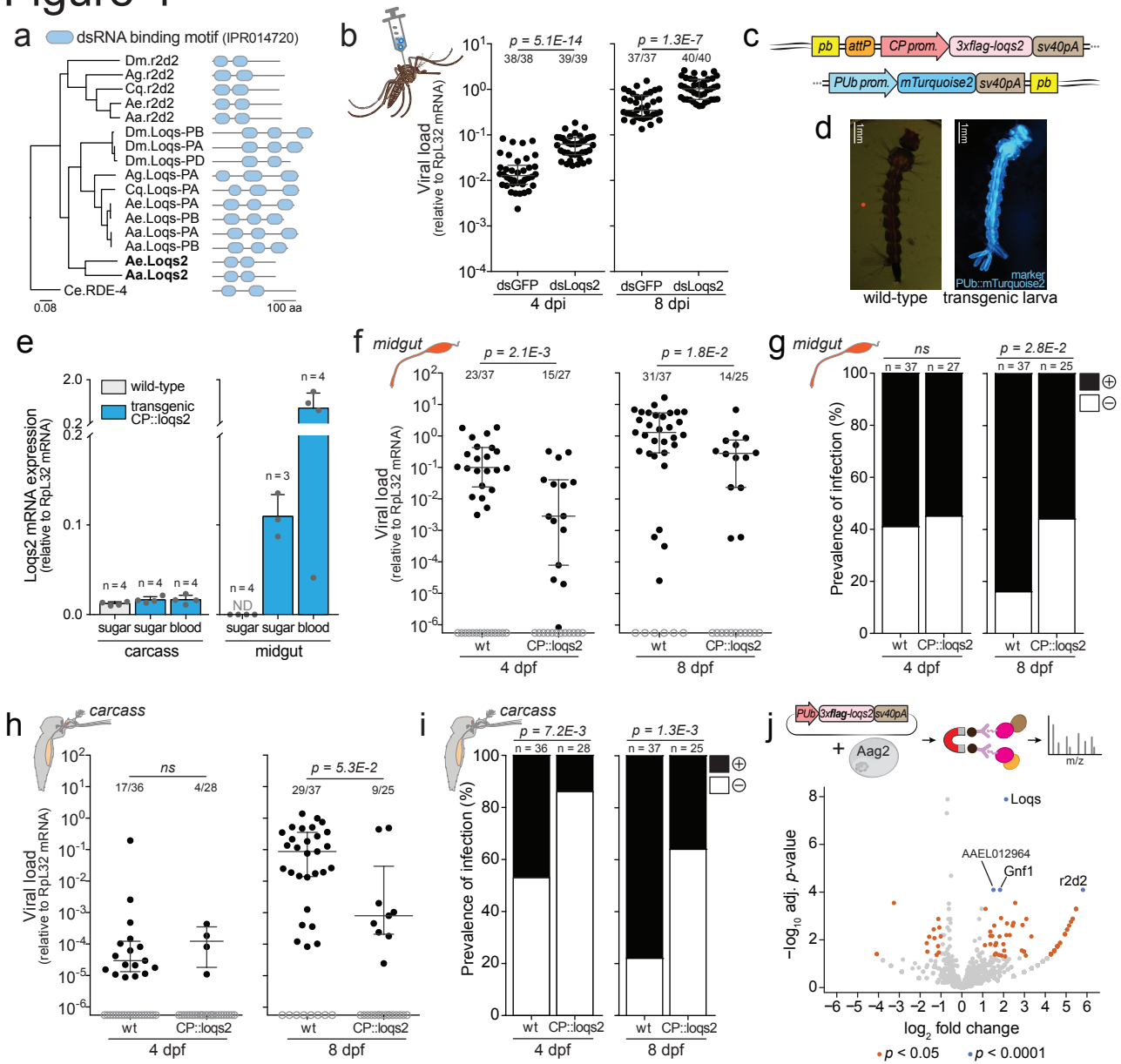
a
dsRNA binding motif (IPR014720)
Dm.r2d2
Ag.r2d2
Cq.r2d2
Ae.r2d2
Aa.r2d2
Dm.Loqs-PB
Dm.Loqs-PA
Dm.Loqs-PD
Ag.Loqs-PA
Cq.Loqs-PA
Ae.Loqs-PA
Ae.Loqs-PB
Aa.Loqs-PA
Aa.Loqs-PB
Ae.Loqs2
Aa.Loqs2
Ce.RDE-4
0.08
100 aa
b
p = 5.1E-14
38/38
39/39
p = 1.3E-7
37/37
40/40
Viral load
(relative to RpL32 mRNA)
dsGFP
dsLoqs2
4 dpi
8 dpi
c
pb
attP
CP prom.
3xflag-loqs2
sv40pA
PUb prom.
mTurquoise2
d
1mm
marker
PUb::mTurquoise2
wild-type
transgenic larva
e
wild-type
transgenic CP::loqs2
Loqs2 mRNA expression
(relative to RpL32 mRNA)
n = 4
n = 3
ND
sugar
blood
carcass
midgut
f
midgut
p = 2.1E-3
23/37
15/25
p = 1.8E-2
31/37
14/25
wt
CP::loqs2
4 dpf
8 dpf
g
midgut
ns
p = 2.8E-2
n = 37
n = 27
n = 25
Prevalence of infection (%)
h
carcass
ns
17/36
4/28
p = 5.3E-2
29/37
9/25
i
carcass
p = 7.2E-3
n = 36
n = 28
p = 1.3E-3
n = 37
n = 25
j
PUb
3xflag-loqs2
sv40pA
Aag2
m/z
Loqs
AAEL012964
Gnf1
r2d2
−log10 adj. p-value
log2 fold change
p < 0.05
p < 0.0001